**Supporting Information**

# Ultrathin and Defect-rich Intermetallic $Pd_2Sn$ Nanosheets for Efficient Oxygen Reduction Electrocatalysis

Jiashun Liang,[a, #] Shenzhou Li, [a, #] Yawei Chen,[b] Xuan Liu,[a] Tanyuan Wang,[a] Jiantao Han,[a] Shuhong Jiao,[b] Ruiguo Cao,[b] Qing Li[a, *]

[a]State Key Laboratory of Material Processing and Die & Mould Technology, School of Materials Science and Engineering, Huazhong University of Science and Technology, Wuhan 430074, China.

[b]Key Laboratory of Materials for Energy Conversion Chinese Academy of Science (CAS), Department of Materials Science and Engineering, University of Science and Technology of China, Hefei 230026, China

[#]These authors contributed equally to this work.

*Corresponding Author. E-mail: qing_li@hust.edu.cn

## EXPERIMENTAL SECTION

**Chemicals and Materials.** $Pd(acac)_2$ (98%), $Sn(Buty)_2(acac)_2$ (97%) (acac = aceylacetonate, buty = butylamide), oleylamine (OAm, 90%), citric acid (CA, 99%), hexadecyltrimethylammonium bromide (CTAB, 99%), dioctadecyl dimethyl ammonium chloride (DODAC, 99%), commercial Pd/C (10 wt%) were purchased from Innochem. Isopropanol (AR), hexane (AR), acetate acid (AR), KOH (95%) and $HClO_4$ (70%) were purchased from SINOPHARM GROUP CO.LTD. Commercial Pt/C was purchased from Johnson Matthey (hispec3000, 20 wt%). All chemicals were used without further purification.

**Synthesis of Pd NSs.** 7.8 mg $Pd(acac)_2$, 36 mg CTAB were dissolved in 5 mL OAm at 45 °C. Under CO atmosphere (~ 20 mL $min^{-1}$), the solution was gradually heated to 160 °C (5 °C /min) and kept for 40 min before it was cooled down to room temperature. During heating process, the solution gradually turned black, indicating the formation of Pd NSs. The product was collected by centrifugation at 9000 rpm for 3 min. The product washed three times with hexane/ethanol mixture, and then redispersed in hexane for further use.

**Synthesis of *o*-$Pd_2Sn$ NSs.** Pd NSs redispersed in hexane, 8 uL $Sn(Buty)_2(acac)_2$ and 100 mg CA were dissolved in 5 mL OAm at 45 °C. Under CO atmosphere (~ 20 mL $min^{-1}$), the solution was gradually heated to 170 °C (5 °C /min) and kept for 120 min

before it was cooled down to room temperature. The purification process is the same as that in the synthesis of Pd NSs.

**Synthesis of *d*-$Pd_4Sn$ NSs.** The synthetic procedure was the similar to that of *o*-$Pd_2Sn$ NSs expect that the reaction temperature was 160 °C.

**Synthesis of *o*-$Pd_2Sn$/C NSs and *d*-$Pd_4Sn$/C NSs.** 12 mg Vulcan XC-72 carbon powder was first dispersed in isopropanol/hexane/acetate acid mixture (v/v/v 10/10/1) by sonication. Then, the as-prepared *o*-$Pd_2Sn$ NSs or *d*-$Pd_4Sn$ NSs were added drop-wise. After sonication for another 1h, the product was collected by centrifugation at 9000 rpm and washed with ethanol for three times. After dry in an oven under vacuum at 60 °C, the final product was obtained.

**Electrochemical Measurements.** Electrochemical measurements were performed on Autolab 302 potentiostation (Metrohm). Glassy carbon rotating disk electrode was used as a working electrode, saturated calomel electrode (saturated KCl) as a reference electrode and graphite rod as a counter electrode. All potentials were converted to values with reference to a reversible hydrogen electrode (vs. RHE).

Ink was prepared by dispersing electrocatalysts (Pd/C, Pt/C, *o*-$Pd_2Sn$/C NSs and *d*-$Pd_4Sn$/C NSs) in a mixture of isopropanol and Nafion (5%) (v/v = 1:0.1, 1 mg $mL^{-1}$).

10 or 20 μL of ink was cast on the glassy carbon and dried under ambient condition. The final loading was determined by ICP-MS (6 $ug_{Pd}$ $cm^{-2}$ for *o*-$Pd_2Sn$/C NSs, *o*-$Pd_2Sn$-200/C NSs and *d*-$P_4$dSn/C NSs, 20 $ug_{Pt\ or\ Pd}$ $cm^{-2}$ for Pt/C and Pd/C).

The CV measurements were performed in $N_2$-saturated 0.1 M KOH solutions at a scan rate of 50 mV/s between 0 and 1.0 V (vs. RHE). The ORR measurements were carried out by rotating disk electrode (RDE) in $O_2$-saturated 0.1 M KOH at a rotation rate of 1600 rpm and a sweep rate of 10 mV/s. Kinetic currents were calculated using Koutecky-Levich equation:

$$i_k = \frac{i_l * i_{0.9}}{i_l - i_{0.9}}$$

Where $i_k$ is the kinetic current, $i_l$ limited current and $i_{0.9}$ current at 0.9 V after iR-corretction.

Accelerated durability test was performed at room temperature by applying cyclic sweeps between 0.6 and 1.0 V in $O_2$-saturated 0.1 M KOH at a sweep rate of 100 mV/s. For the CO stripping test, CO gas (99.9%) was first bubbled into 0.1 M KOH while holding the working electrode potential at 0.1 V for 10 min. After purging the electrolyte with $N_2$ for at least 15 min, two CVs (0-1 V) were recorded at a scan rate of 20 mV $s^{-1}$. All of the measurements were carried out at room temperature.

**Characterizations.** TEM images and EDX spectra were collected from a FEI Tecani G2 20 at an operation voltage of 200 kV. HRTEM, and HAADF-STEM images and

EDX mapping were taken from a FEI Tecani G2 F30 and Talos F200X. XRD were collected from Rigaku MiniFlex 600 diffractometer with a Cu radiation source (λ = 0.15406 nm). XPS spectra were collected from AXIS-ULTRA DL*D*-600W. ICP-MS result was carried out from ELAN DRC-e. AFM were conducted on Bruker Dimension Icon in the PeakForce tapping mode.

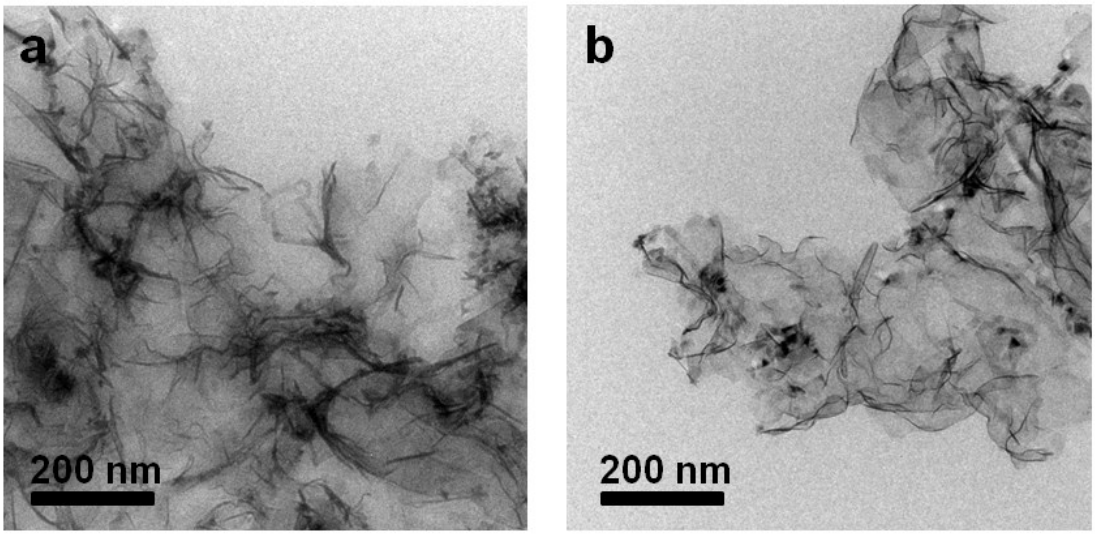


**Figure S1**. Additional TEM images of Pd NSs.

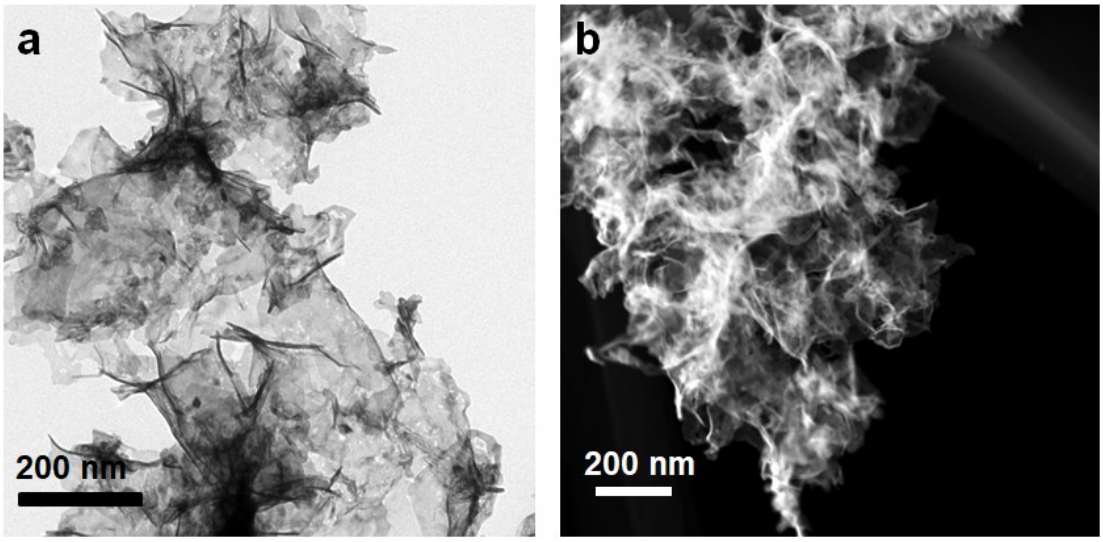


**Figure S2.** Additional TEM and HAADF-STEM images of *o*-$Pd_2Sn$ NSs.

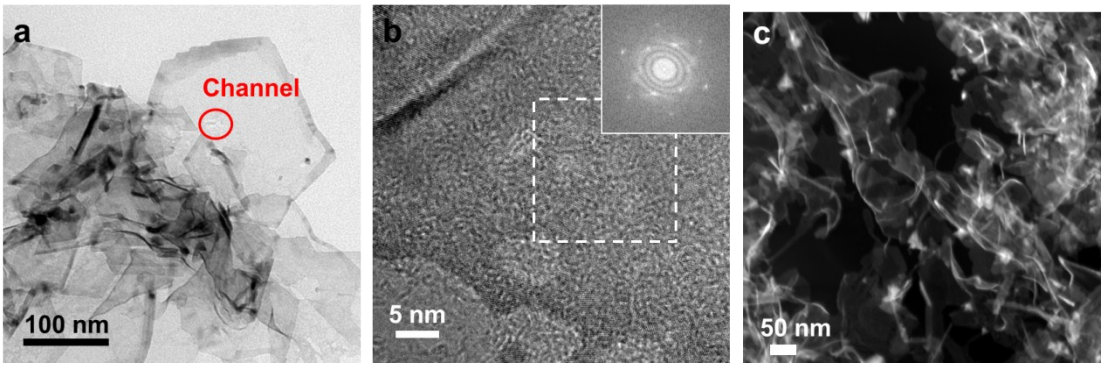


**Figure S3.** (a) TEM, (b) HRTEM, and (c) HAADF-STEM images of *d*-$Pd_4Sn$ NSs.

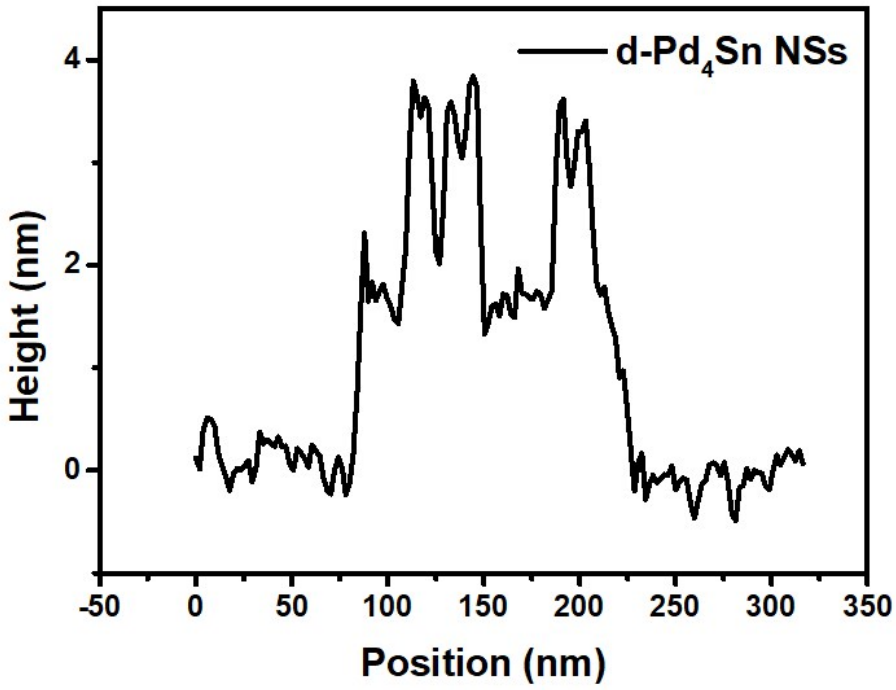


**Figure S4.** AFM height profiles of *d*-$Pd_4Sn$ NSs

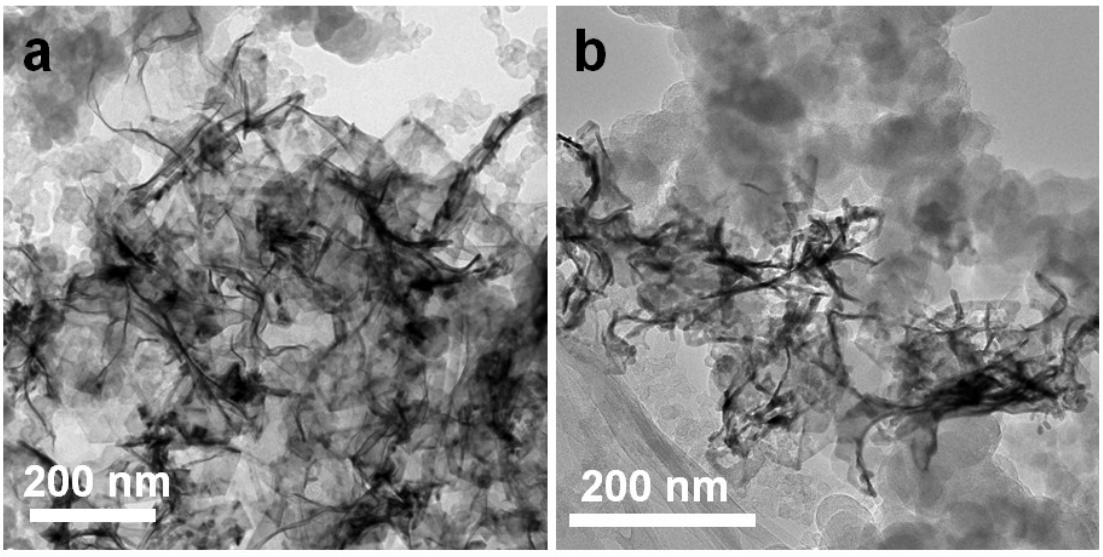


**Figure S5.** TEM images of (a) *d*-$Pd_4Sn$ NSs/C and (b) *o*-$Pd_2Sn$/C.

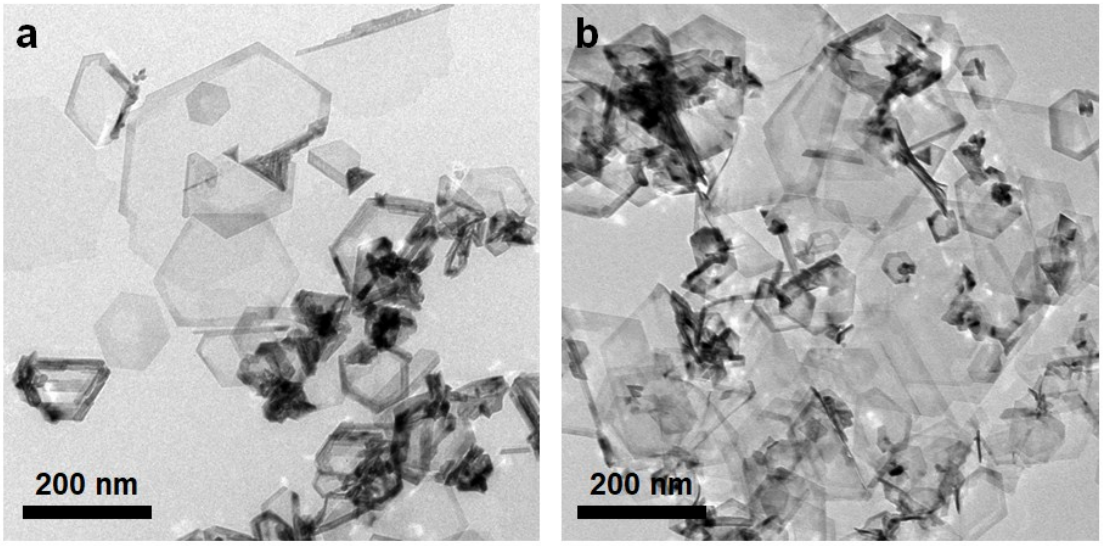


**Figure S6.** TEM images of (a) Pd NSs prepared in the absence of CTAB, (b) Pd NSs prepared by replacing CTAB with DODAC.

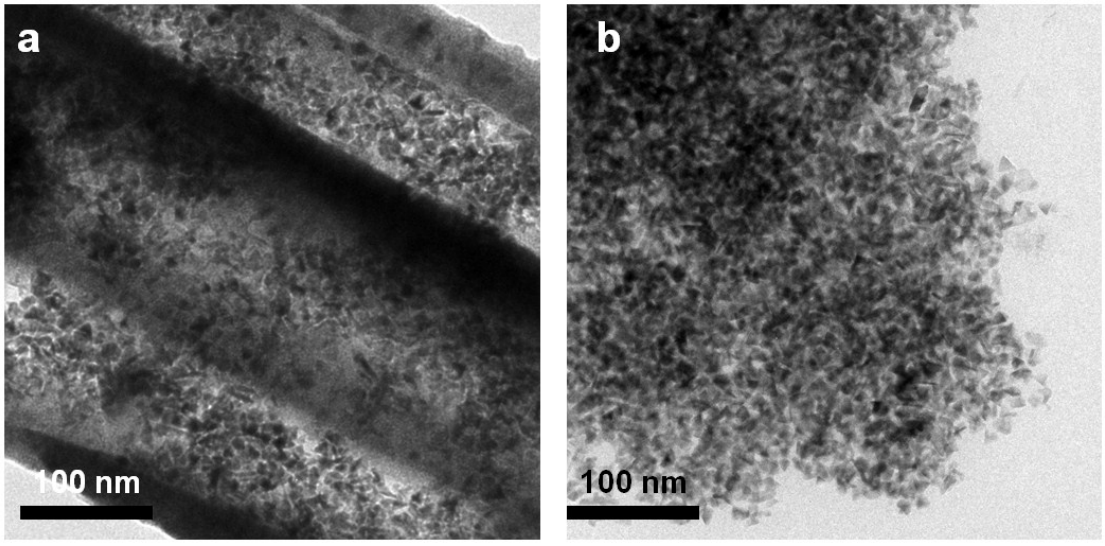


**Figure S7.** TEM images of *o*-$Pd_2Sn$ NSs prepared using one-pot method.

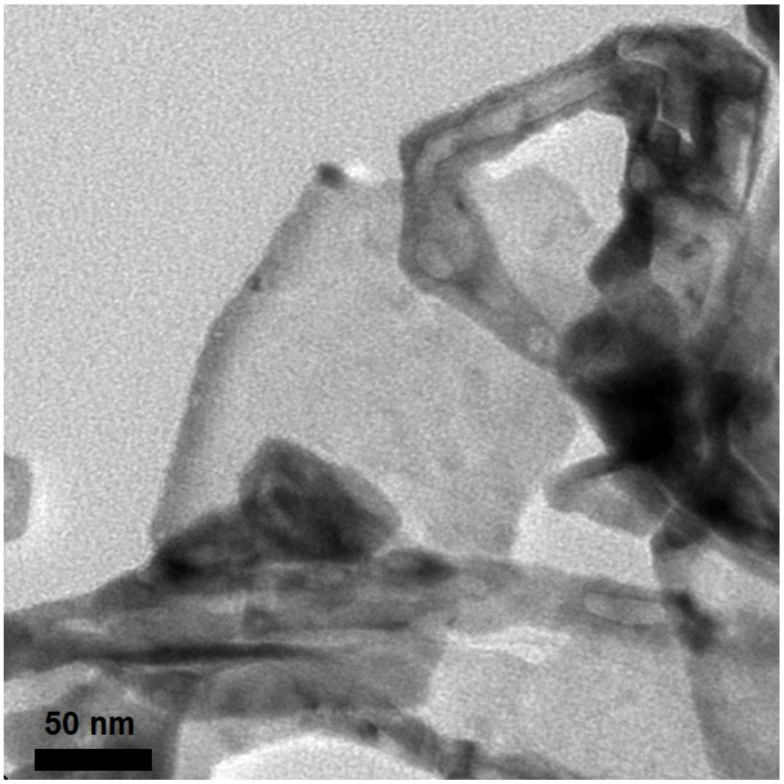


**Figure S8.** TEM image of *o*-$Pd_2Sn$ NSs prepared at 200 °C.

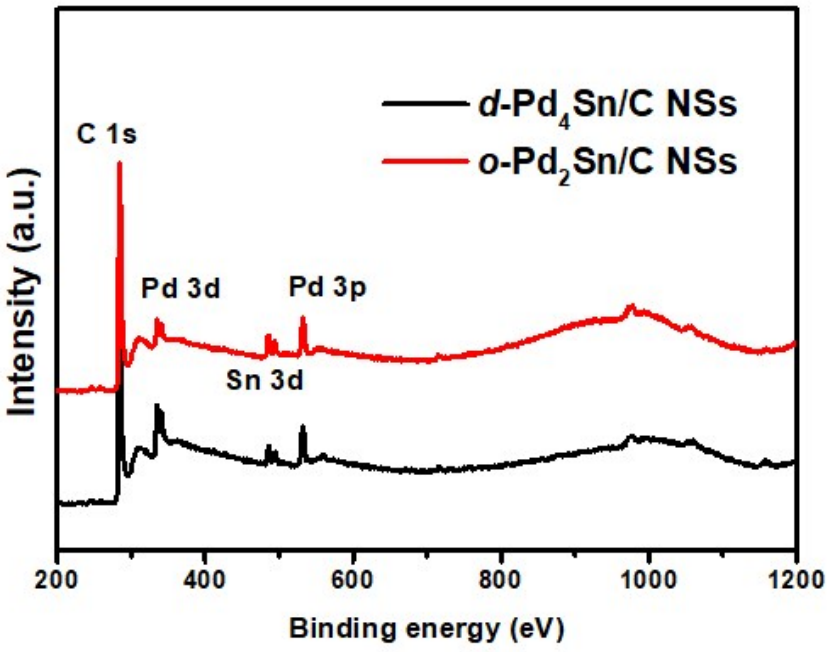

**Figure S9.** XPS survey spectra of *d*-PdSn/C and *o*-$Pd_2Sn$/C.

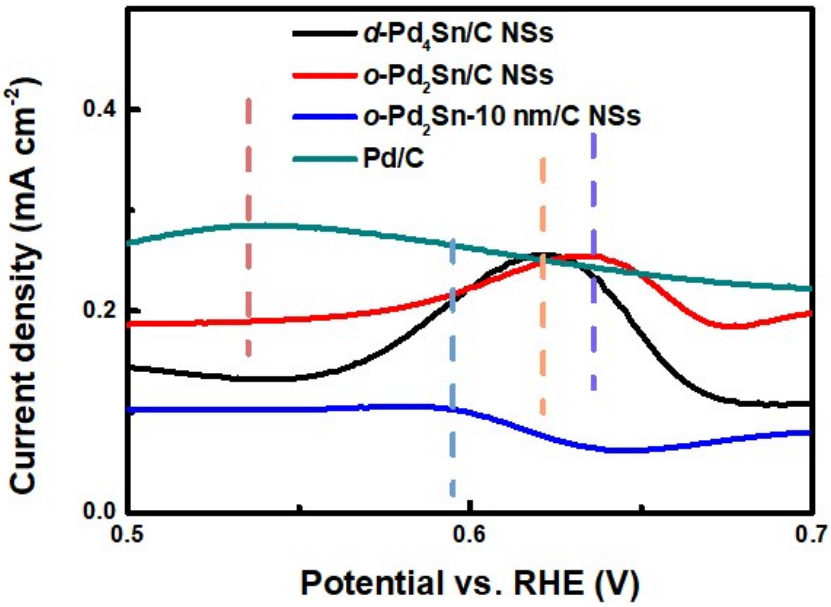


**Figure S10.** Enlarged CV curves of *d*-$Pd_4Sn$/C NSs, *o*-$Pd_2Sn$/C NSs, *o*-$Pd_2Sn$-200/C NSs and Pd/C at the range of 0.5-0.7 V.

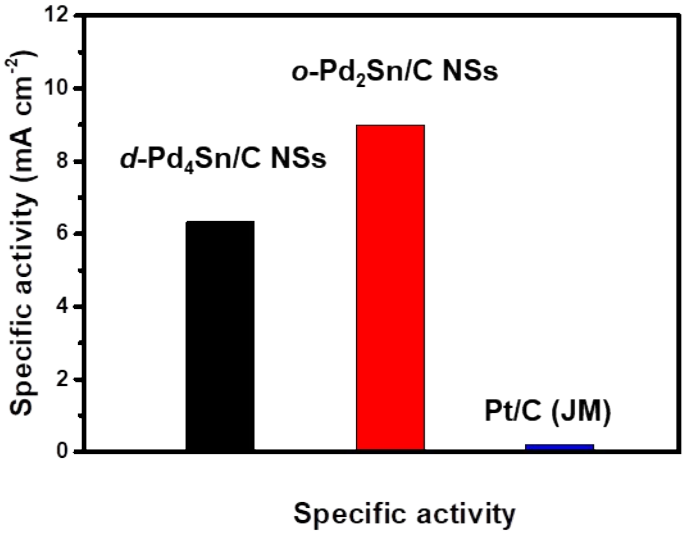

**Figure S11.** Specific activity of *d*-$Pd_4Sn$/C and *o*-$Pd_2Sn$/C NSs for ORR at 0.9 $V_{iR\text{-free}}$.

(Note: The ECSA of Pt/C was evaluated in $N_2$-saturated 0.1 M $HClO_4$.)

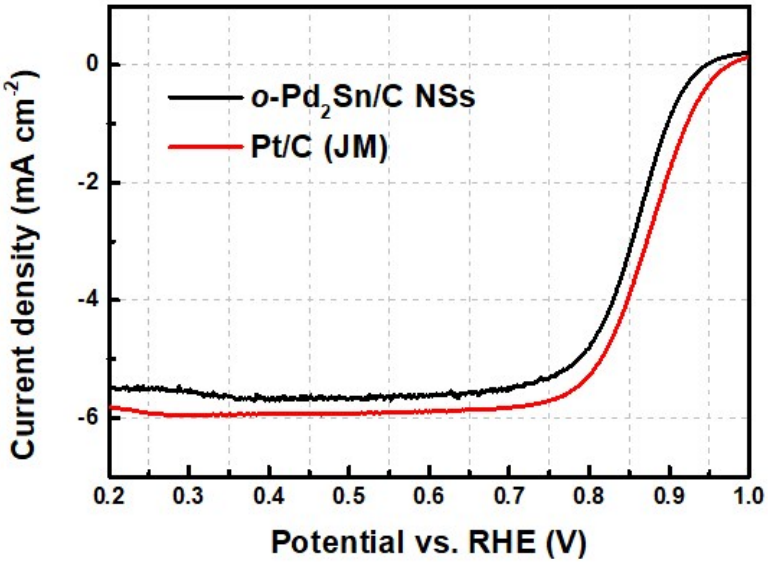


**Figure S12.** ORR polarization curves of *o*-$Pd_2Sn$/C NSs and Pt/C in $O_2$-saturated 0.1 M $HClO_4$, 10 mV/s, 1600 rpm, 20 $ug_{Pt\ or\ Pd}\ cm^{-2}$ for *o*-$Pd_2Sn$/C NSs and Pt/C.

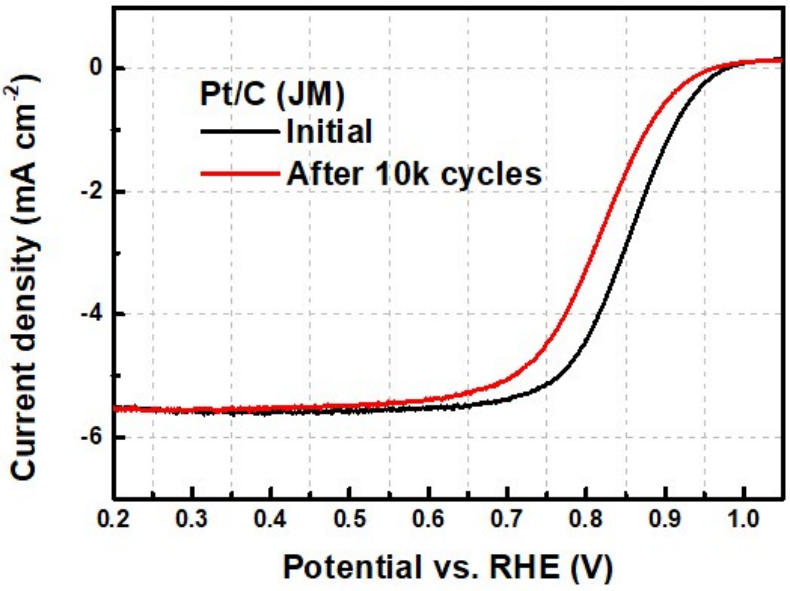


**Figure S13.** ORR polarization curves of Pt/C before and after stability tests in $O_2$-saturated 0.1 M KOH.

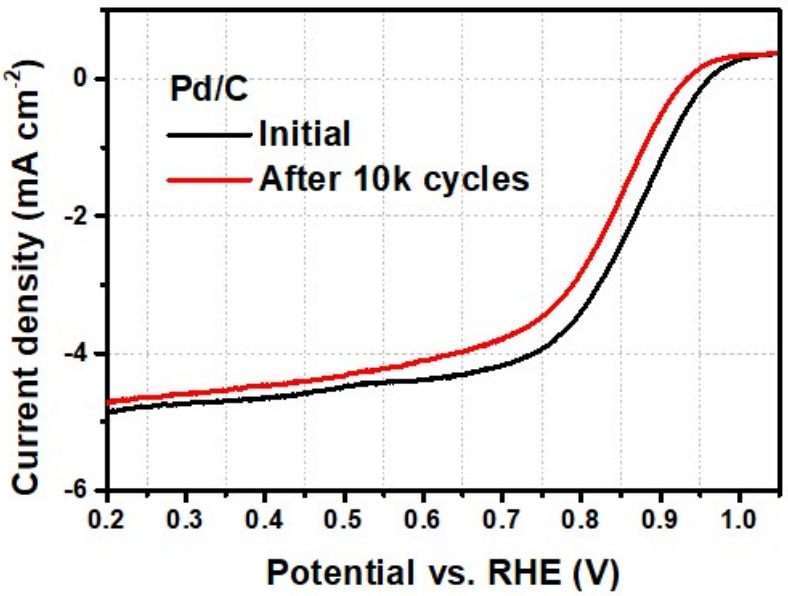


**Figure S14.** ORR polarization curves of Pd/C before and after stability tests in $O_2$-saturated 0.1 M KOH.

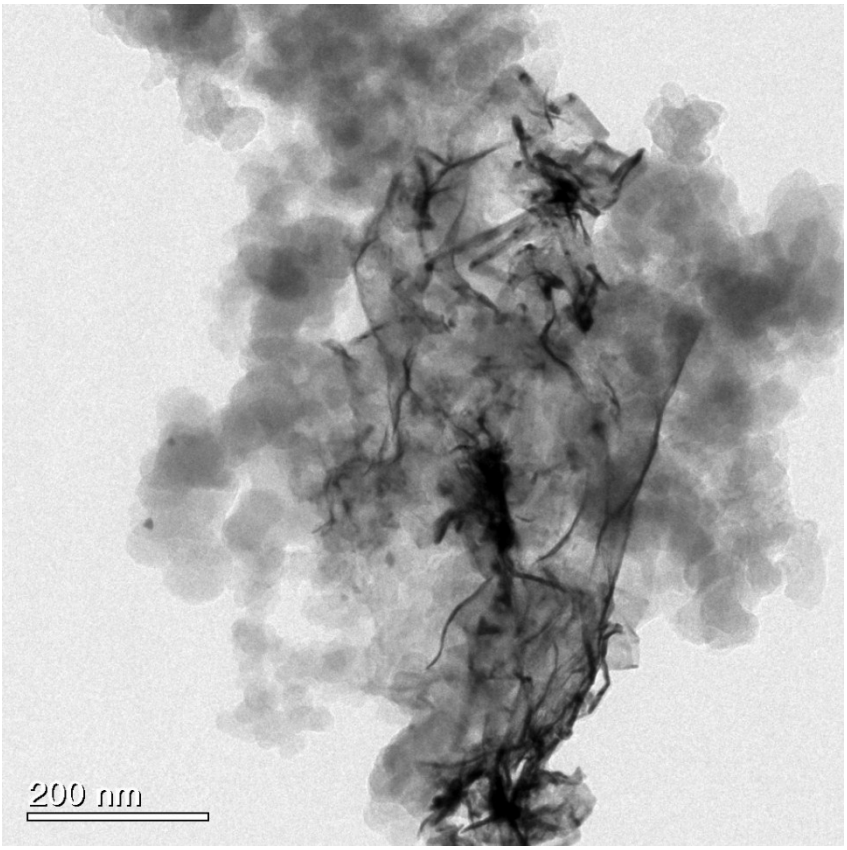


**Figure S15.** TEM image of *o*-$Pd_2Sn$/C NSs after stability test.

**Table S1.** Comparison of ORR activity of the reported electrocatalysts in 0.1 M KOH.

| Electrocatalysts | MA @ 0.9 V ($A\ mg_{PGM}^{-1}$) | SA @ 0.9 V ($mA\ cm^{-2}$) | $E_{1/2}$ (V) | Reference |
|---|---|---|---|---|
| *o*-$Pd_2Sn$/C NSs | 2.5 | 9 | 0.893 | This work |
| PdMo bimetallene/C | 16.37 | 11.64 | 0.95 | [1] |

| | | | | |
|---|---|---|---|---|
| Pd NSs 5ML/C | 8.07 | 10.91 | 0.95 | [1] |
| $Pt_{32}Pd_{48}Ni_{20}$ NSs/C | 0.57 | N/A | ~0.87 | [2] |
| $Pd_3Pb$/Pd NSs | 0.574 | 1.31 | ~0.9 | [3] |
| $Pd_3Bi$/C NPs | 1.2 | 2.3 | ~0.9 | [4] |
| $Pd_{31}Bi_{12}$/C NPs | 0.95 | 2.45 | 0.92 | [5] |
| Pd/PdFe NPs | 0.31 | 1.56 | ~0.89 | [6] |
| $Pd_3Pb$ Tripods | 0.56 | 1.76 | ~0.9 | [7] |
| $Pd_3Pb$ Nanoflowers | 1.14 | 4.71 | ~0.91 | [8] |
| PtPdCo NanoRings/C | 3.58 | 4.91 | 0.966 | [9] |

## References


1. M. C. Luo, Z. L. Zhao, Y. L. Zhang, Y. J. Sun, Y. Xing, F. Lv, Y. Yang, X. Zhang, S. Hwang, Y. N. Qin, J. Y. Ma, F. Lin, D. Su, G. Lu and S. J. Guo, *Nature*, 2019, **574**, 81-+.
2. J. P. Lai, F. Lin, Y. H. Tang, P. Zhou, Y. G. Chao, Y. L. Zhang and S. J. Guo, *Adv. Energy Mater.*, 2019, **9**, 1800684.
3. C. Y. Tang, N. Zhang, Y. J. Ji, Q. Shao, Y. Y. Li, X. H. Xiao and X. Q. Huang, *Nano Lett.*, 2019, **19**, 1336-1342.

4. D. Sun, Y. F. Wang, K. J. T. Livi, C. H. Wang, R. C. Luo, Z. Q. Zhang, H. Alghamdi, C. Y. Li, F. F. An, B. Gaskey, T. Mueller and A. S. Hall, *ACS Nano*, 2019, **13**, 10818-10825.

5. Y. F. Wang and A. S. Hall, *Acs Energy Lett*, 2020, **5**, 17-22.

6. X. Li, X. Li, C. Liu, H. Huang, P. Gao, F. Ahmad, L. Luo, Y. Ye, Z. Geng and G. Wang, *Nano Lett.*, 2020, DOI: 10.1021/acs.nanolett.9b05024.

7. L. Z. Bu, Q. Shao, Y. C. Pi, J. L. Yao, M. C. Luo, J. P. Lang, S. Hwang, H. L. Xin, B. L. Huang, J. Guo, D. Su, S. J. Guo and X. Q. Huang, *Chem-Us*, 2018, **4**, 359-371.

8. S. Luo, Y. Ou, L. Li, J. J. Li, X. Q. Wu, Y. Jiang, M. X. Gao, X. F. Yang, H. Zhang and D. R. Yang, *Nanoscale*, 2019, **11**, 17301-17307.

9. Y. J. Sun, X. Zhang, M. C. Luo, X. Chen, L. Wang, Y. J. Li, M. Q. Li, Y. N. Qin, C. J. Li, N. Y. Xu, G. Lu, P. Gao and S. J. Guo, *Adv. Mater.*, 2018, **30**, 1802136.